MOLECULAR IMAGING AND BIOLOGY

Mol Imaging Biol (2015) 17:214–221
DOI: 10.1007/s11307-014-0796-2

Published Online: 4 October 2014

RESEARCH ARTICLE

Sodium [^{18}F]Fluoride PET/CT in Myocardial Infarction

Jeong Hee Han,[1] Sue Yeon Lim,[1] Min Su Lee,[1] Won Woo Lee[1,2]

[1]*Department of Nuclear Medicine, Seoul National University Bundang Hospital, Seoul National University College of Medicine, 173-82 Gumi-ro, Bundang-gu, Seongnam-si, Gyeonggi-do, 463-707, Republic of Korea*
[2]*Institute of Radiation Medicine, Medical Research Center, Seoul National University, 101 Daehak-ro, Jongno-gu, Seoul, 110-744, Republic of Korea*

Abstract
Purpose: Sodium [^{18}F]fluoride (Na[^{18}F]F) positron emission tomography with integrated computed tomography (PET/CT) has not been used for imaging myocardial infarction (MI). Here, we aimed to investigate the Na[^{18}F]F PET/CT features of MI in a rat model.
Procedures: MI was induced by coronary artery ligation in 8-week-old male Spraque–Dawley rats (300±10 g) and confirmed by triphenyl tetrazolium chloride (TTC) staining. Na[^{18}F]F PET/CT images were obtained using an animal-dedicated PET/CT scanner (NanoPET/CT, Mediso) *in vivo* and *ex vivo*. Uptake of Na[^{18}F]F was quantitated using the standardized uptake value (SUV). Myocardial apoptosis was evaluated using histone-1 targeted peptide (ApoPep-1) and terminal deoxynucleotidyl transferase dUTP nick end labeling (TUNEL) staining, while calcium accumulation was investigated using von Kossa's staining. Na[^{18}F]F PET/CT was compared with ^{99m}Tc-methoxyisobutylisonitrile (MIBI) or ^{99m}Tc-hydroxymethylenediphosphonate (HMDP) single photon emission computed tomography/computed tomography (SPECT/CT) in rats with day 1 MI.
Results: The rats showed strong Na[^{18}F]F uptake both *in vivo* and *ex vivo*; the maximal uptake occurred 1 day after MI (SUV ratio of infarct to lung = 4.56±0.74, n=7, P=0.0183 vs the control). The Na[^{18}F]F uptake area perfectly matched the apoptotic area, determined by ApoPep-1 uptake and TUNEL assay. However, calcification, assessed by von Kossa's staining, was absent in the infarct. Na[^{18}F]F PET/CT showed an increased uptake at the perfusion deficit area in [^{99m}Tc]MIBI SPECT/CT and an equivalent signal to [^{99m}Tc]HMDP SPECT/CT in rats with day 1 MI.
Conclusions: Na[^{18}F]F PET/CT is a promising hot-spot imaging modality for MI.

Key words: ^{18}F-sodium fluoride, Positron emission tomography, Computed tomography, Myocardial infarction, Apoptosis, Calcification

Introduction

Sodium [^{18}F]fluoride (Na[^{18}F]F) is a radiopharmaceutical agent with strong bone affinity and is suited for positron emission tomography (PET) [1, 2]. A variety of bone diseases, whether benign or malignant, have been successfully evaluated using Na[^{18}F]F PET with or without integrated computed tomography (CT) [3–6]. In addition, soft tissue uptake of Na[^{18}F]F has been reported in malignant diseases such as lung cancer, renal cell cancer, and metastatic brain tumor and in benign diseases including myositis ossificans, choroid plexus calcification, and coronary atherosclerosis [7, 8]. Myocardial infarction (MI) was investigated using the old positron scintillation camera technology in 1979 [9], but, to the best of our knowledge,

Correspondence to: Won Woo Lee; *e-mail:* wwlee@snu.ac.kr

Na[^{18}F]F has never been applied to MI imaging using the current state-of-the-art PET/CT fusion technology, which would enable highly accurate delineation of MI. In this study, we aimed to investigate the Na[^{18}F]F PET/CT features of MI in a rat model.

Materials and Methods

Rat Model of MI

MI was induced by coronary artery ligation in 8-week-old male Sprague–Dawley (SD) rats weighing 300±10 g. In brief, rats were anesthetized by intraperitoneal injection of 0.3 ml of a 3:2 (*v/v*) mixture of tiletamine–zolazepam (50 mg/ml Zoletil, Virbac) and xylazine (23 mg/ml Rompun, Bayer). After intubation under ventilator control (model 683, Harvard Apparatus), supplying 2–5l/min of oxygen, the thoracic cage was cut through the sternum to expose the heart. At the level of the auricular appendage, the left anterior descending coronary artery was ligated with 4–0 silk sutures (Woori Medical). Blood flow impairment and the subsequent discoloration were always confirmed in the myocardium just distal to the ligation site. Then, the sternum and overlying skin were closed with 2–0 silk sutures (Ethicon). Control rats underwent a sham operation, without coronary ligation. The institutional animal welfare committee approved the animal experiments.

Na[^{18}F]F PET/CT

Na[^{18}F]F was obtained through the (p,n) reaction of ^{18}O in an in-house cyclotron (Kotron13, Samyoung Unitech) and injected (dose = 11.1–18.5 MBq) into the tail vein. An animal-dedicated scanner (NanoPET/CT, Mediso) was used for imaging under inhalation anesthesia (2–3 % of isoflurane in 2–5 l/min of oxygen) [10].

CT images were obtained first with the following parameters: projection number of 240, pitch of 1, tube voltage of 55 kVp, tube current of 145 μA, exposure time of 1,100 ms, and CT dose index of 9.0 cGy. Image acquisition lasted for 13 min and iodinated contrast (Ultravist370, Bayer) was infused (3 ml for 10 min) using an auto-injector (NanoJet, Revodix) during the CT acquisition. The CT images were reconstructed using the following parameters: Butterworth filter, matrix of 332×332×473, and voxel size of 211×211×211 μm. The CT spatial resolution was 48 μm.

Then, 30 min after the injection of Na[^{18}F]F, PET images were acquired for 30 min using the following parameters: axial field of view (FOV) of 94.7 mm (1 bed), 1–5 acquisition coincidence mode, and coincidence time window of 5 ns. The sinogram of the images was reconstructed using the iterative 3D EM adjoint Monte Carlo algorithm. The image matrix was 110×110×234 and voxel size was 0.4×0.4×0.4 mm. The spatial resolution of the reconstructed images was 1.2 mm.

After the *in vivo* image acquisition, rats were euthanized, and the hearts were harvested and sectioned into 1-mm-thick myocardial rings using a slicer (rat heart section mold, Zivic Instruments). The myocardial rings were imaged for 1 h to obtain *ex vivo* PET/CT images using the same acquisition and reconstruction parameters as for *in vivo* PET/CT.

PET/CT Image Analysis

The degree of Na[^{18}F]F uptake was quantitated using nuclear imaging software (PMOD 3.13, PMOD Technologies) in terms of the standardized uptake value (SUV), as follows: SUV = (decay-corrected radioactivity in mCi/ml)×(weight of rat in grams)/(injected radioactivity in mCi). The SUVs of the infarct and lung were calculated in spherical regions of interest (ROIs) with 2-mm radii and expressed as a ratio. The *ex vivo* radioactivities of the infarct and a remote area were also assessed in spherical ROIs with 2-mm radii.

Analysis of Apoptosis

Apoptosis-targeting peptide (ApoPep-1) [11] conjugated with red fluorescent dye (AHR-553, BioActs) was used to demonstrate myocardial apoptosis. The peptide probe had excitation and emission wavelengths of 561 and 589 nm, respectively. It was injected (100 nmol; 100 μl of 1-mM stock solution in dimethyl sulfoxide and double-distilled water) 2 h before the rats were euthanized. After *in vivo* and *ex vivo* Na[^{18}F]F PET/CT as already described, the myocardial rings were also imaged in a fluorescence imaging system (Lumina II, PerkinElmer) using the channels of 535 nm for excitation and 583 nm for emission. The *ex vivo* fluorescence signals of the infarct and a remote area were assessed using built-in software (Living Image 4.3.1).

TTC Staining

For this experiment, rats were euthanized, the abdomen was opened, and the inferior vena cava (IVC) was exposed. First, 30 ml of normal saline was infused through the IVC to perfuse the circulatory system. Then, the thoracic cage was opened, the ascending aorta was identified, and 30 ml of the 2 % solution of 2,3,5-triphenyl-2H-tetrazolium chloride (TTC) was infused through the ascending aorta into the left ventricle (LV) and thus the coronary system. Thereafter, the heart was excised and incubated in 4 % paraformaldehyde solution for 1 h at 37 °C with light protection. Finally, 1-mm-thick myocardial rings were obtained using the slicer (rat heart section mold, Zivic Instruments) and scanned with a flatbed scanner (HP Scanjet G4010, Hewlett-Packard).

TUNEL Staining

For terminal deoxynucleotidyl transferase (TdT) dUTP nick end labeling (TUNEL) assay, a commercial kit (In Situ Cell Death Detection kit, POD, Roche) was used. In brief, 4-μm-thick myocardial sections were deparaffinized, washed in a graded series of ethanol, and rehydrated. The sections were fixed in 4 % paraformaldehyde in phosphate-buffered saline (PBS) for 15 min, washed two times in PBS, and incubated at room temperature for 30 min with proteinase K solution. Then, equilibrium buffer was applied at room temperature. TdT

reaction mix was applied for 60 min at 37 °C in a humidified chamber. The reaction was stopped using 2× saline-sodium citrate (SSC) buffer for 15 min, and the sections were washed in PBS, 0.3 % hydrogen peroxide for 5 min, and PBS again. Streptavidin–horseradish peroxidase (HRP) conjugate (Roche) was applied to the sections at room temperature for 30 min followed by 3,3′-diaminobenzidine (DAB, Roche) staining. Finally, the sections were immersed several times in deionized water and mounted.

Analysis of Calcification

Von Kossa′s staining was employed for evaluating calcium deposition. Paraffin-embedded myocardial tissues were sectioned into 4-μm-thick slices, deparaffinized, and hydrated. Then, 5 % silver nitrate solution was applied and the slices were placed in front of a 60-W lamp for 1 h. After the slices were washed three times in distilled water, 5 % hypo was applied for 5 min. After washing in water again, the slices were dehydrated and coverslipped.

SPECT/CT versus PET/CT

Because the traditional test for MI imaging in nuclear medicine is either cold-spot [^{99m}Tc]methoxyisobutylisonitrile ([^{99m}Tc]MIBI) or hot-spot [^{99m}Tc]hydroxymethylenediphosphonate ([^{99m}Tc]HMDP) [12, 13] gamma camera imaging, direct comparisons between [^{99m}Tc]MIBI/[^{99m}Tc]HMDP single photon emission computed tomography (SPECT)/CT and Na[^{18}F]F PET/CT were performed. The rats with day 1 MI underwent [^{99m}Tc]MIBI or [^{99m}Tc]HMDP SPECT/CT followed by Na[^{18}F]F PET/CT 2 h later. The SPECT/CT images were obtained using an animal-dedicated scanner (NanoSPECT/CT, Bioscan), enabling high-resolution multi-pinhole SPECT acquisition. First, CT images were acquired using the following parameters: scan length 4.4 cm, projection 240, pitch 1, X-ray tube voltage 45 kVp, tube current 18.8 mAs, and CT dose index 120 mGy. Iodinated contrast agent was not used due to the concern of volume overload of total injected fluid. The CT raw data were reconstructed using a cone beam filtered back projection algorithm with a low-pass filter (Shepp-Logan, cutoff frequency of 50 %) into 0.2×0.2×0.2 mm^3 voxel images. After CT image acquisition, SPECT was conducted 1 h post-injection of [^{99m}Tc]MIBI or [^{99m}Tc]HMDP (dose = 37 MBq, each). The SPECT system consisted of four detectors, each having a pyramidal collimator with 9 pinhole (2.5-mm diameter) aperture on top, enabling 36 pinhole SPECT images. Using a step-and-shoot acquisition mode, three-dimensional scintigraphic images were acquired for 30 min covering 4.4-cm scan length of thorax with 15° angular increment, 18 projections per detector, and 90-s acquisition per projection. The acquired SPECT raw data were reconstructed into 0.2×0.2×0.2 mm^3 voxel images using an iterative algorithm. SPECT/CT images were analyzed and fused with PET/CT images on the nuclear imaging software (PMOD 3.13, PMOD Technologies).

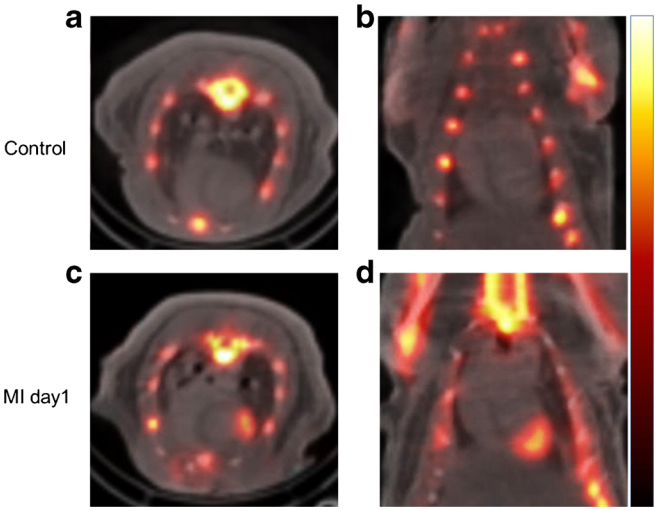

Fig. 1 Na[^{18}F]F PET/CT images *in vivo* obtained 24 h after coronary artery ligation. After Na[^{18}F]F injection via the tail vein (dose = 18.5 MBq), PET/CT images were acquired using the animal-dedicated scanner (NanoPET/CT, Mediso) under inhalation anesthesia (2–3 % isoflurane in 2–5 l/min of oxygen). CT images were first acquired and then PET images were obtained 30 min after the injection of Na[^{18}F]F. Compared with the control rat (**a**, **b**), the rat with MI readily shows strong uptake of Na[^{18}F]F in the infarct (**c**, **d**). Panels **a** and **c** are transaxial images, and panels **b** and **d** are coronal images.

Statistical Analysis

Data are presented as the mean ± SEM. The Mann–Whitney *U* test and Bonferroni correction were used to analyze SUV ratios.

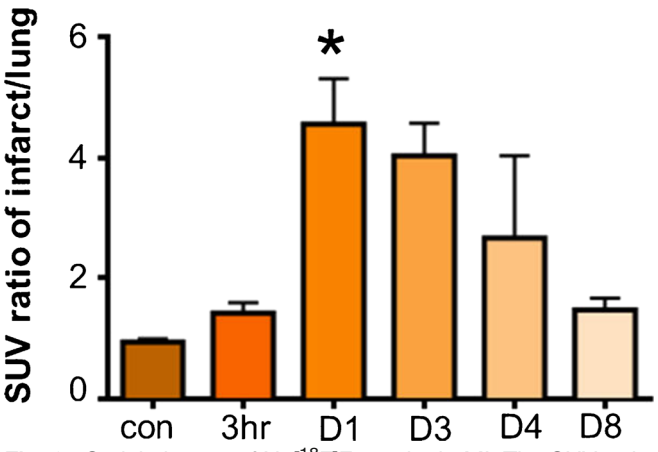

Fig. 2 Serial change of Na[^{18}F]F uptake in MI. The SUV ratio of infarct to lung began increasing as early as 3 h (1.42±0.17, n=4), peaked on day 1 (4.56±0.74, p=0.0183, n=7), decreased on day 3 (4.03±0.54, n=3), further decreased on day 4 (2.66±1.37, n=2), and reached the 3-h level on day 8 (1.48 ±0.20, n=2) after MI. Data are the mean ± SEM of the number of rats. *P=0.0183 compared with the control (0.94± 0.05, n=4).

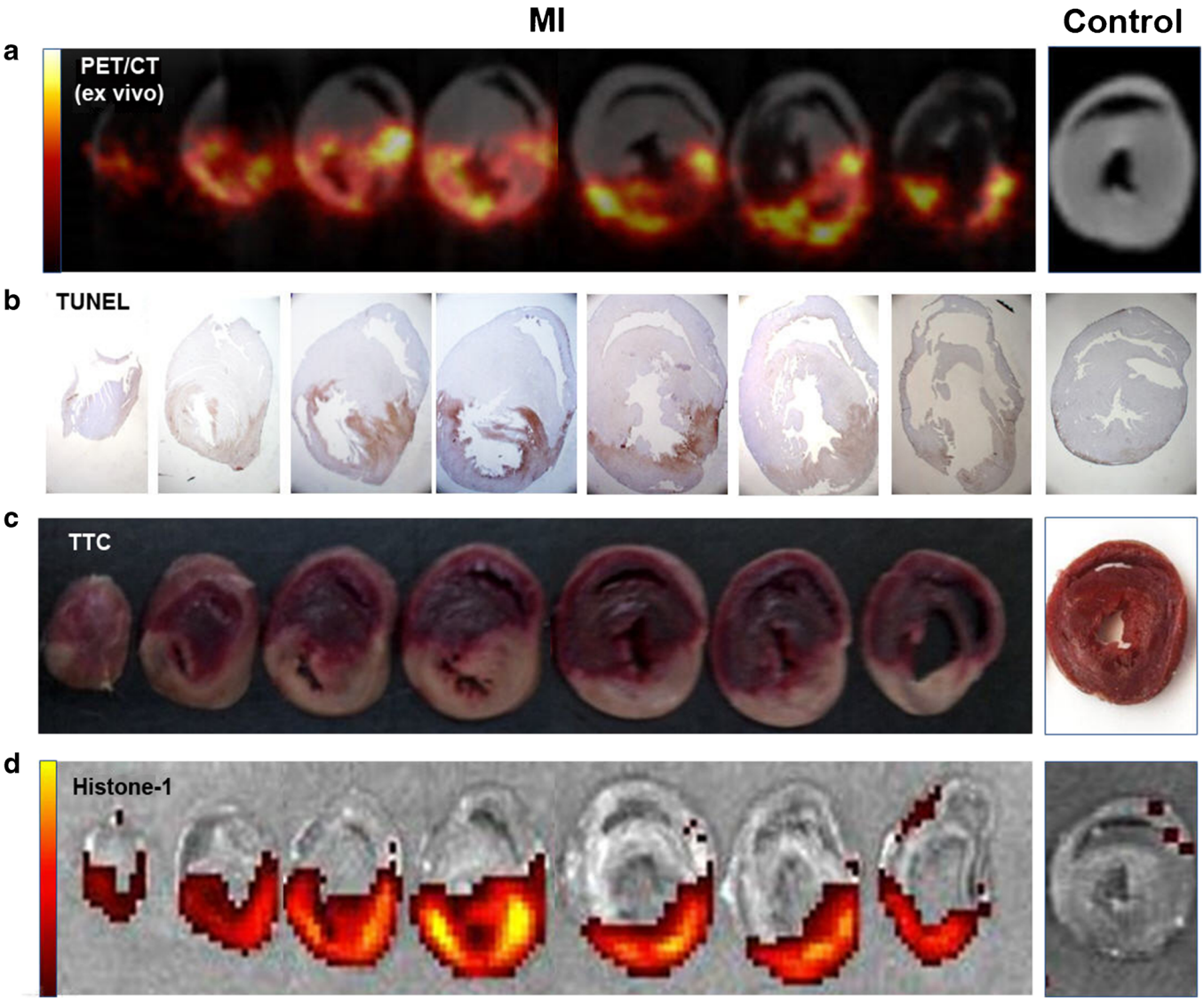

Fig. 3 Na[^{18}F]F PET/CT images *ex vivo*. The strong uptake of Na[^{18}F]F in the infarct noted by *in vivo* PET/CT was also recapitulated by *ex vivo* PET/CT (**a**). TUNEL staining results (**b**) were closely associated with those of Na[^{18}F]F-positive area. Furthermore, the infarct area with TTC-negative (**c**) and histone-1-positive (**d**) findings was strongly correlated with Na[^{18}F]F uptake.

Statistical software (PASW Statistics 18.0.0, IBM) was used for all the analyses. $P<0.05$ was considered statistically significant.

Results

Na[^{18}F]F PET/CT In Vivo

The *in vivo* PET/CT images revealed strong uptake of Na[^{18}F]F in the infarct (Fig. 1). Na[^{18}F]F uptake began as early as 3 h, reached the maximal level at 1 day ($P=0.0183$), decreased at 3 days, further decreased at 4 days, and almost returned to the 3-h level at 8 days after MI. The corresponding SUV ratios of infarct to lung were as follows: control, 0.94±0.05; 3 h, 1.42±0.17; day 1, 4.56±0.74; day 3, 4.03±0.54; day 4, 2.66±1.37; and day 8, 1.48±0.20 (Fig. 2).

Na[^{18}F]F Uptake Ex Vivo

The TUNEL staining positive area was almost perfectly matched with Na[^{18}F]F-positive area in the *ex vivo* PET/CT images. Furthermore, the TTC-negative and histone-1-positive infarct area was strongly associated with Na[^{18}F]F uptake (Fig. 3). On the other hand, von Kossa's calcium staining was negative in the same area (Fig. 4). Quantitative analysis also revealed the close relationship between Na[^{18}F]F uptake and histone-1 expression. In the *ex vivo* PET/CT images, the radioactivity ratio of infarct to remote area was 32.8±4.7, which was significantly greater than that

of control rats (0.96±0.12, P=0.0025). The fluorescence signal ratio of infarct to remote area was 30.3±2.6, which was also significantly higher than that of control rats (0.99±0.11, P<0.0001). Therefore, the infarct had similar degrees of Na[18F]F uptake and histone-1 expression when compared with the remote area (Fig. 4).

SPECT/CT Versus PET/CT

Perfusion impairment, the indirect evidence of MI, was readily appreciated in [99mTc]MIBI SPECT/CT on day 1 after MI, and Na[18F]F uptake was observed in the same perfusion deficit area (Fig. 5). In addition, Na[18F]F PET/CT has signal distribution similar to [99mTc]HMDP SPECT/CT, the traditional hot-spot imaging modality for infarct (Fig. 6).

Discussion

Na[18F]F PET/CT has been successfully applied in a variety of cardiovascular diseases [14, 15]. Coronary atherosclerosis [7], aortic valve stenosis [16], and global cardiovascular calcification [17, 18] are the reported clinical utilities of Na[18F]F PET/CT. However, to our knowledge, MI has never been investigated using the state-of-the-art Na[18F]F PET/CT technique. In the current study, we demonstrate that MI could be successfully visualized using Na[18F]F PET/CT. Na[18F]F uptake in infarct was closely associated with myocardial apoptosis but not with calcification. Na[18F]F PET/CT was positive at the perfusion deficit area in [99mTc]MIBI SPECT/CT and showed almost the same signal distribution with [99mTc]HMDP SPECT/CT.

Hot-spot imaging in MI has been realized using Tc-99m-labeled phosphorous agents such as [99mTc]pyrophosphate

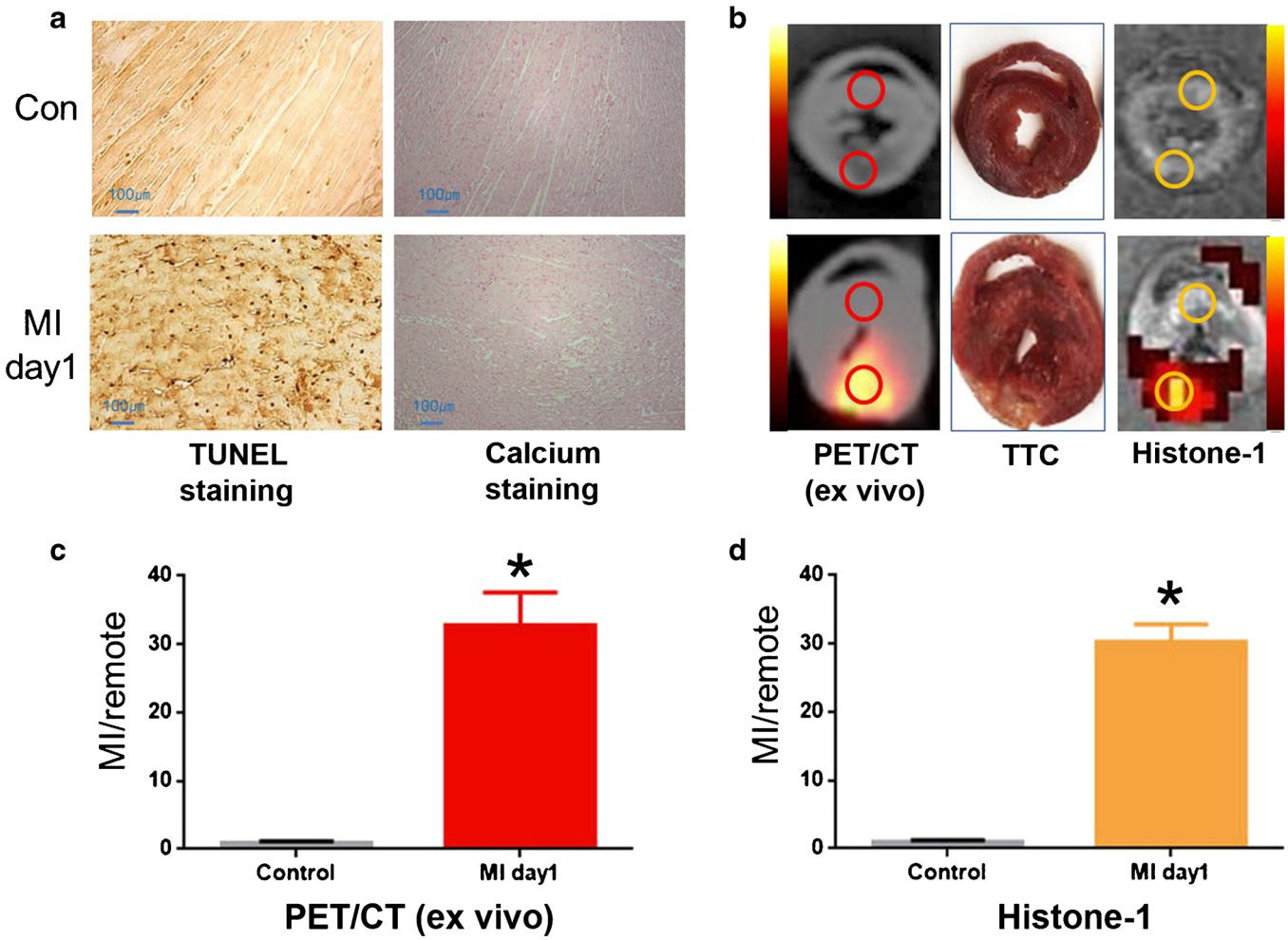

Fig. 4 The relationships of Na[18F]F uptake with apoptosis, calcium accumulation, and histone-1 expression. **a** TUNEL assay demonstrated DNA fragmentation, the hallmark of apoptosis, in the infarct, whereas von Kossa's staining, for calcium accumulation, was negative in the same area. **b** *Ex vivo* PET/CT images of myocardial rings showed intense uptake of Na[18F]F in the TTC-negative area, which was strongly positive for histone-1 expression. *Red circles* in the *ex vivo* PET/CT images indicate spherical ROIs with 2-mm radii; radioactivity was expressed in kBq/ml. *Yellow circles* in the histone-1-positive images indicate planar ROIs with 2-mm radii; the fluorescence signal was expressed in photons/s/sr/cm^2. **c** The radioactivity ratio of infarct to remote area was 32.8±4.7 (mean ± SEM; n=3–4), and **d** the fluorescence ratio of infarct to remote area was 30.3±2.6 (mean±SEM; n=3–4). *P<0.01 compared with the controls (Color figure online).

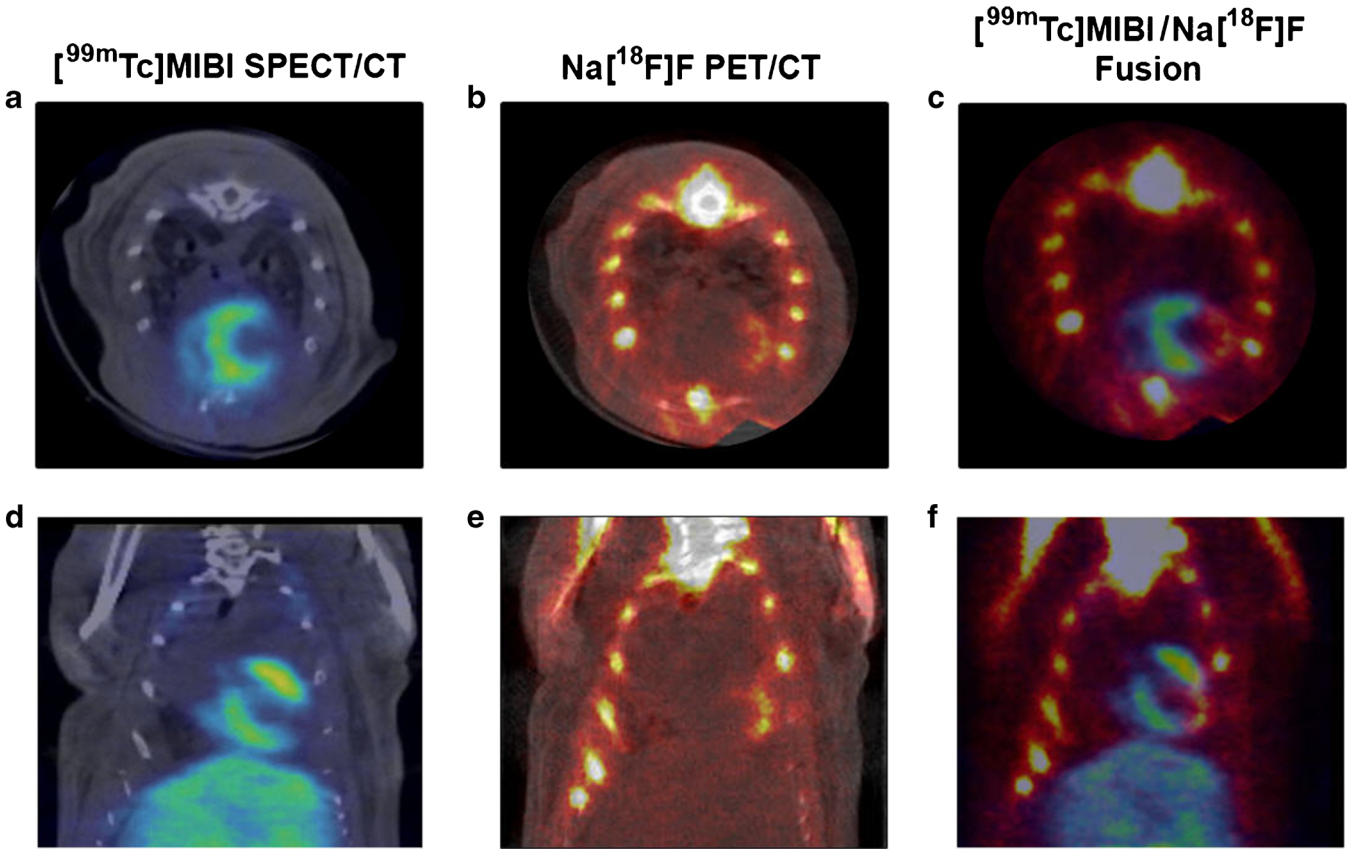

Fig. 5 Comparison of [^{99m}Tc]MIBI SPECT/CT and Na[^{18}F]F PET/CT images of a rat 1 day after MI. [^{99m}Tc]MIBI SPECT/CT and Na[^{18}F]F PET/CT were serially performed in a 2-h interval. Perfusion impairment was readily observed in the apico-lateral area (**a**, **d**), where Na[^{18}F]F uptake was positive (**b**, **e**). The fusion images of [^{99m}Tc]MIBI SPECT and Na[^{18}F]F PET show the close association between the perfusion impairment and Na[^{18}F]F uptake (**c**, **f**). Iodinated contrast was not used for the CT acquisitions. Panels **a**, **b,** and **c** are transaxial images, and panels **d**, **e,** and **f** are coronal images.

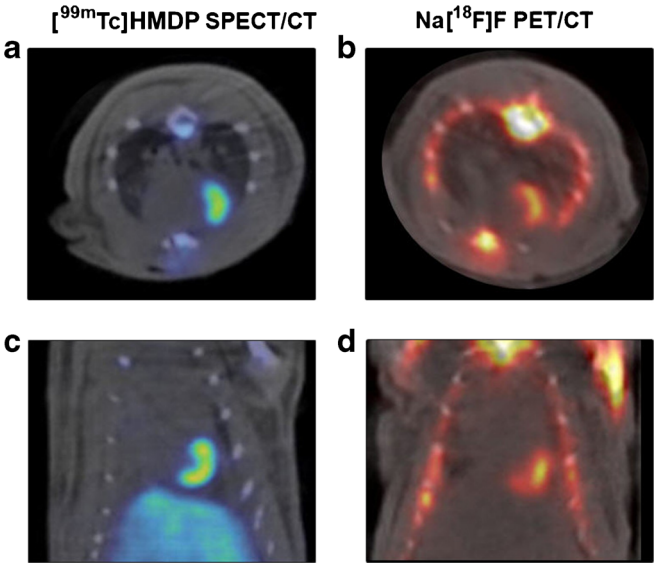

Fig. 6 Comparison of [^{99m}Tc]HMDP SPECT/CT and Na[^{18}F]F PET/CT images of a rat 1 day after MI. [^{99m}Tc]HMDP SPECT/CT and Na[^{18}F]F PET/CT were serially performed in a 2-h interval. The rat showed almost the same distribution of [^{99m}Tc]HMDP (**a**, **c**) and Na[^{18}F]F (**b**, **d**). Iodinated contrast was not used for the CT acquisitions. Panels **a** and **b** are transaxial images, and panels **c** and **d** are coronal images.

[19], [^{99m}Tc]methylenediphosphonate (MDP) [13], or [^{99m}Tc]HMDP [12]. However, ^{18}F-NaF PET/CT has advantages over Tc-99m-based gamma camera imaging. First, the resolution of the PET image is better than that of the SPECT image. Second, the robust attenuation correction algorithm of PET, which is absent in gamma camera imaging, can lead to accurate quantitation of biomarker signals, as represented by the high correlation of Na[^{18}F]F uptake with myocardial expression of histone-1 (Fig. 4). Third, the fast pharmacokinetics of Na[^{18}F]F should enable MI imaging in a reasonably short time [1]; Na[^{18}F]F PET/CT is completed in less than 1 h from the injection, but Tc-99m-based gamma camera imaging requires more than 2 h. Lastly, the radioactivity used in Na[^{18}F]F PET/CT is usually one third to one fifth that in Tc-99m-based gamma camera imaging in the clinical situations, potentially reducing patient exposure to radiation [2, 7], although the higher photon energy of F-18 (511 KeV) beta positron than that of Tc-99m (140 KeV) gamma photon should be considered for accurate determination of the radiation hazard.

ApoPep-1 interacts with histone-1 that is translocated from the nucleus to the cell membrane during the early

apoptotic process [11]. The greater the uptake of ApoPep-1 in MI, the poorer the functional outcome post-MI [20]. In comparison with annexin V, which requires calcium for its target binding, ApoPep-1 can bind to histone-1 in calcium-free conditions [11]. In fact, one interesting finding of the current study was that Na[^{18}F]F uptake in the infarct was not associated with calcium accumulation. Therefore, the mechanism of Na[^{18}F]F uptake in MI may be different from that in bone. In other words, the formation of fluoroapatite [$Ca_{10}(PO_4)_6(F)_2$], through the ion exchange between the hydroxyl moiety of hydroxyapatite [$Ca_{10}(PO_4)_6(OH)_2$] and the [^{18}F]fluoride ion, may play a minimal role for Na[^{18}F]F uptake in MI. Na[^{18}F]F uptake in MI, therefore, may occur in several different ways. First, Na[^{18}F]F may directly interact with histone-1 on the surface of injured cells [20]. Because of its high positive charge, specifically via the high lysine content in the C-terminal, histone-1 usually resides in the nucleus and interacts with DNA, which is negatively charged [21]. Ischemic cell injury releases histone-1 from the nucleus to the sarcoplasmic membrane, where it may directly interact with the [^{18}F]fluoride anion. In this regard, Na[^{18}F]F PET/CT holds great promise for the early detection of myocardial apoptosis because histone-1 translocation has been reported in the early apoptotic process [22]. Second, Na[^{18}F]F may contribute to the formation of calcium-free fluorophosphates such as isoflurophate [$C_6H_{14}FO_3P$] (http://en.wikipedia.org/wiki/Diisopropyl_fluorophosphate) in conditions of high phosphatase activity and great amount of inorganic phosphate, which has often been suggested to exist in MI [23]. Lastly, the amount of calcium deposition after MI may be less than the detectable range of von Kossa's staining, and Na[^{18}F]F may still bind to the small amount of calcium crystals that cannot be detected by the staining method [24]. This issue needs further investigation.

Limitations

Na[^{18}F]F PET/CT may have some limitations for the early detection of MI, because the highest uptake of Na[^{18}F]F occurs as late as 1 day after MI (Fig. 2). As a matter of fact, late visualization of MI is the critical drawback of Tc-99m-labeled phosphorous agents [12, 13, 19]. In this regard, the clinical utility of Na[^{18}F]F PET/CT remains questionable. In the authors' opinion, the usefulness of Na[^{18}F]F PET/CT in cardiovascular disease may lie in the visualization of reversible ischemic injury. For example, visualization of the area at risk by Na[^{18}F]F PET/CT in ischemia-reperfusion injury would have a tremendous impact on the management of patients with acute coronary syndrome [25]. This issue is now being investigated in our institute.

Conclusion

MI could be successfully visualized using Na[^{18}F]F PET/CT. Na[^{18}F]F uptake was closely associated with myocardial apoptosis but not with calcification. Na[^{18}F]F PET/CT was positive at the perfusion deficit area in [^{99m}Tc]MIBI SPECT/CT and showed almost the same signal distribution with [^{99m}Tc]HMDP SPECT/CT. These findings suggest that Na[^{18}F]F PET/CT is a promising hot-spot imaging modality for MI.

Acknowledgments. This study was supported in part by a grant of the Korean Health Technology R&D Project, Ministry of Health & Welfare, Republic of Korea (A111627-1101-0000100), by grants from the National Research Foundation (NRF), Ministry of Education, Science and Technology (MEST), Republic of Korea (2012M2B2A9A02029612; 2012M2A2A7035589; 2014M2B2A9030104); Basic Science Research Program, 2012R1A1A2001060; and Global Core Research Center (GCRC) program, 2011–0030680, and by grant of the SNUBH Research Fund (02-2013-035).

Conflict of interest. There is no conflict of interest to declare.

Ethical approval. All applicable institutional and national guidelines for the care and use of animals were followed.

Funding Source. This study was supported in part by a grant of the Korean Health Technology R&D Project, Ministry of Health & Welfare, Republic of Korea (A111627-1101-0000100), by grants from the National Research Foundation (NRF), Ministry of Education, Science and Technology (MEST), Republic of Korea (2012M2B2A9A02029612; 2012M2A2A7035589; 2014M2B2A9030104); Basic Science Research Program, 2012R1A1A2001060; and Global Core Research Center (GCRC) program, 2011–0030680), and by grant of the SNUBH Research Fund (02-2013-035).

References

1. Grant FD, Fahey FH, Packard AB et al (2008) Skeletal PET with ^{18}F-fluoride: applying new technology to an old tracer. J Nucl Med 49:68–78
2. Lee SJ, Lee WW, Kim SE (2013) Bone positron emission tomography with or without CT is more accurate than bone scan for detection of bone metastasis. Korean J Radiol 14:510–519
3. Schirrmeister H, Guhlmann A, Elsner K et al (1999) Sensitivity in detecting osseous lesions depends on anatomic localization: planar bone scintigraphy versus ^{18}F PET. J Nucl Med 40:1623–1629
4. Kang JY, Lee WW, So Y et al (2010) Clinical usefulness of ^{18}F-fluoride bone PET. Nucl Med Mol Imaging 44:55–61
5. Hetzel M, Arslandemir C, Konig HH et al (2003) F-18 NaF PET for detection of bone metastases in lung cancer: accuracy, cost-effectiveness, and impact on patient management. J Bone Miner Res 18:2206–2214
6. Yoon S-H, Kim KS, Kang SY et al (2013) Usefulness of ^{18}F-fluoride PET/CT in breast cancer patients with osteosclerotic bone metastases. Nucl Med Mol Imaging 47:27–35
7. Dweck MR, Chow MW, Joshi NV et al (2012) Coronary arterial 18F-sodium fluoride uptake: a novel marker of plaque biology. J Am Coll Cardiol 59:1539–1548
8. Sheth S, Colletti PM (2012) Atlas of sodium fluoride PET bone scans: atlas of NaF PET bone scans. Clin Nucl Med 37:e110–e116
9. Cochavi S, Pohost GM, Elmaleh DR, Strauss HW (1979) Transverse-sectional imaging with Na^{18}F in myocardial infarction. J Nucl Med 20:1013–1017
10. Szanda I, Mackewn J, Patay G et al (2011) National Electrical Manufacturers Association NU-4 performance evaluation of the PET component of the NanoPET/CT preclinical PET/CT scanner. J Nucl Med 52:1741–1747
11. Wang K, Purushotham S, Lee JY et al (2010) In vivo imaging of tumor apoptosis using histone H1-targeting peptide. J Control Release 148:283–291
12. Bevan JA, Tofe AJ, Benedict JJ, Francis MD, Barnett BL (1980) Tc-99m HMDP (hydroxymethylene diphosphonate): a radiopharmaceutical for skeletal and acute myocardial infarct imaging. II. Comparison of Tc-99m hydroxymethylene diphosphonate (HMDP) with other technetium-

labeled bone-imaging agents in a canine model. J Nucl Med 21:967–970
13. Huckell VF, Lyster DM, Morrison RT, Cooper JA (1985) Comparison of technetium-99m pyrophosphate and technetium-99m methylene diphosphonate with variable amounts of stannous chloride in the detection of acute myocardial infarction. Clin Nucl Med 10:455–462
14. Mohler ER 3rd, Alavi A, Wilensky RL (2012) (18)F-fluoride imaging for atherosclerosis. J Am Coll Cardiol 60:1711–1712
15. Chen W, Dilsizian V (2013) Targeted PET/CT imaging of vulnerable atherosclerotic plaques: microcalcification with sodium fluoride and inflammation with fluorodeoxyglucose. Curr Cardiol Rep 15:364
16. Hyafil F, Messika-Zeitoun D, Burg S et al (2012) Detection of 18fluoride sodium accumulation by positron emission tomography in calcified stenotic aortic valves. Am J Cardiol 109:1194–1196
17. Beheshti M, Saboury B, Mehta NN et al (2011) Detection and global quantification of cardiovascular molecular calcification by fluoro18-fluoride positron emission tomography/computed tomography–a novel concept. Hell J Nucl Med 14:114–120
18. Basu S, Hoilund-Carlsen PF, Alavi A (2012) Assessing global cardiovascular molecular calcification with ^{18}F-fluoride PET/CT: will this become a clinical reality and a challenge to CT calcification scoring? Eur J Nucl Med Mol Imaging 39:660–664
19. Rude RE, Parkey RW, Bonte FJ et al (1979) Clinical implications of the technetium-99m stannous pyrophosphate myocardial scintigraphic "doughnut" pattern in patients with acute myocardial infarcts. Circulation 59:721–730
20. Acharya B, Wang K, Kim IS et al (2013) In vivo imaging of myocardial cell death using a peptide probe and assessment of long-term heart function. J Control Release 172:367–373
21. Harshman SW, Young NL, Parthun MR, Freitas MA (2013) H1 histones: current perspectives and challenges. Nucleic Acids Res 41:9593–9609
22. Ohsawa S, Hamada S, Yoshida H, Miura M (2008) Caspase-mediated changes in histone H1 in early apoptosis: prolonged caspase activation in developing olfactory sensory neurons. Cell Death Differ 15:1429–1439
23. Park JB, Kang DY, Yang HM et al (2013) Serum alkaline phosphatase is a predictor of mortality, myocardial infarction, or stent thrombosis after implantation of coronary drug-eluting stent. Eur Heart J 34:920–931
24. Rungby J, Kassem M, Eriksen EF, Danscher G (1993) The von Kossa reaction for calcium deposits: silver lactate staining increases sensitivity and reduces background. Histochem J 25:446–451
25. Leuschner F, Panizzi P, Chico-Calero I et al (2010) Angiotensin-converting enzyme inhibition prevents the release of monocytes from their splenic reservoir in mice with myocardial infarction. Circ Res 107:1364–1373